Gif-sur-Yvette,

01/06/2016

Dear Editor,

We have answered to the referees' comments and modified consequently the paper as discussed in the detailed answers. We hope that the paper is now suitable for publication in ESD and we thanks the referees for their interesting comments/remarks which have surely improved the quality of our works.

Best Regards,

Davide Faranda & Dimitri Defrance

Anonymous Referee #1

Overall quality. This is a good paper, with some limitations as to the broader conclusions. The authors apply new wavelet based metrics on the changes in circulation under a changing climate and the use of these novel diagnostics is the strongest part of this paper. However, the authors have applied this methodology to a coarse resolution atmospheric simulation that may not be adequate to draw all of the conclusions stated in the paper. This flaw can be rectified, however, by reducing the scope of the conclusions for reasons stated below.

This paper has three main parts: 1) the use of a wavelet filter to separate the coherent and turbulent components of the 700 hPa wind field; 2) The analysis of these fields using two novel metrics in a simulation of the present day climate; 3) the analysis of the changes in these metrics in future climates simulate using RCP 2.5 and RCP 8.5 warming scenarios.

There are questions with respect to the implementation of the first part and the interpretation of the third part. With respect to the implementation of the first part the, filter and separation, the concern is that the turbulent component has a large seasonal cycle contribution; as large as the coherent part of the flow. This appears to be an inadequacy of the filter since one would assume that there should be only a small contribution from seasonal fluctuations in the turbulent component. It would be comforting if the authors at least noted this problem in the paper.

We discuss this issue in the new version of the manuscript by adding: "The limits of the wavelet filtering technique appear by looking at the spectral peak corresponding to the seasonal cycle which cannot be completely eliminated, although it represents a coherent component of the signal." Our considerations were mostly related to the slope of the spectrum.

Second, the authors interpret the analysis of their results indicating a relative increase in the coherent component versus the turbulent component under the RCP 8.5 scenario as pointing to an increase in predictability. This may be true, however, only for the scales that are well resolved in the IPSLCM5-LR model used; i.e. structures on the synoptic and planetary scales well resolved by a 3.75°x1.875° mesh. This says nothing about what may happen to meso-scale and convective scale phenomena that are unresolvable with such a coarse resolution as used here.

The reviewer is right in saying that we have to focus our conclusions on the synoptic and planetary scales resolved by the model. We have understated the results in the new version of the paper. We also includes some new analyses at Medium Resolution (see supplementary material) which add an

interesting point to what observed by the referee: increasing the resolution causes also a relative increase of ΔY of u700 and ΔΛ of v700 component (see supplementary material). This means that turbulent contributions become more relevant as finer scales are included in the analysis, although the scale of the analysis still remains much larger than the scales of convective structures.

Technical corrections :

Pg 2 line 16 ' only change the intensity' should be ' only a change in the intensity'

Pg 4 line 4 'an higher' should be 'a higher' Pg 4 line 31 'At the tropics' should be 'In the tropics'

Pg 5 line 6 'ibn' should be 'in' Discussion paper

Pg 5 line 21 'hilited by an alternance' should be 'highlighted by an alteration'

Pg 5 line 29 'of about' should be ' by about'

The typos will be corrected in the new version of the paper

Anonymous Referee #2

The wavelet-based approach is up to my knowledge a novel methodology for analyzing climate models, though it has been used for image or reservoir reconstructions. I, however, have big doubts that this method is suitable for climatology. Climate modeling demands multi-scale modeling as well but the scale separation is often difficult to de- fine and what is more important there is a multi-scale interaction that evolves in time. Therefore, the method should be first rigorously examined for climate models (starting from toy models and propagating towards more complex models) before drawing the conclusions about the climate system itself.

The wavelet approach has been devised for analyzing turbulent signals containing non-trivial scale separations. The original paper by Farge (1992) contains applications of wavelet filtering for toy models as well as for turbulent complex systems. This paper has, up to date, ~1500 citations, corresponding to just as many applications in complex fluid mechanics. The technique is not new to climate sciences as well: Torrence and Compo published in 1998 "a practical guide to wavelet analysis" in BAMS. This article is cited 7000 times. Wavelets have also been applied to the analysis of geophysical time series by several authors (Grinsted et al 2004, Ghil 2002,…). This vast literature explains why we did not include any validations of the methodology for toy models.

In the previous version of the paper we gave just a short introduction to the wavelet methods. We admit that, as the reviewer suggests, we could give more precise references on how the technique has been already validated in climate science. This justifies why we did not do any validation study. The new version contains a more extended review of the relevant wavelet climate-related literature.

We want also to remark that the paper is not about wavelet filtering that we take for granted for the reasons specified above. The wavelet filtering is here used to separate coherent and turbulent components. The originality of our analysis lies in analyzing these components separately.

References (included in the new version of the manuscript)

-Torrence, Christopher, and Gilbert P. Compo. "A practical guide to wavelet analysis." ***Bulletin of the American Meteorological society*** **79.1 (1998): 61-78.**

-Grinsted, Aslak, John C. Moore, and Svetlana Jevrejeva. "Application of the cross wavelet transform and wavelet coherence to geophysical time series."*Nonlinear processes in geophysics* 11.5/6 (2004): 561-566.

-Ghil, Michael, et al. "Advanced spectral methods for climatic time series."*Reviews of geophysics* 40.1 (2002).

Authors claim that the integral of the ACF detects the predictability. However, for that not only the correlation should be high but the error should be small, which is not shown.

The link between Correlations decay and predictability is well known in dynamical systems, although this result has not been applied so often (or sometimes just implicitly) to climate science. Some supplementary references can be found in:

-Osborne, A. Ro, and A. Provenzale. "Finite correlation dimension for stochastic systems with power-law spectra." *Physica D: Nonlinear Phenomena* 35.3 (1989): 357-381.

-Govindan, R. B., K. Narayanan, and M. S. Gopinathan. "On the evidence of deterministic chaos in ECG: Surrogate and predictability analysis." *Chaos: An Interdisciplinary Journal of Nonlinear Science* 8.2 (1998): 495-502.

-Crisanti, A., et al. "Intermittency and predictability in turbulence." *Physical review letters* 70.2 (1993): 166.

Since this literature is probably unknown in climate science, we give such references in the new version of the manuscript.

Authors test the metrics on one resolution model. However, one needs to show that the wavelet-based separation gives satisfactory results by considering models with different resolutions.

This is a good suggestion for validating our metrics. We performed several tests on higher resolution simulation, namely the medium resolution version of the IPSL model (MR) and compared the results to the low resolution model (LR) analyzed in the previous version of the manuscript. Results are nicely consistent between the two resolutions and we report them in the new supplementary data of the manuscript. The analysis also shows that the spatial structures of the indicators are similar.

Authors claim that the difference between $\Lambda 2055{-}2105$ and $\Lambda 2005{-}2055$ detects the predictability. I am wondering about sensitivity of this metric with respect to the time interval.

The reviewer also suggests to perform a sensitivity study with respect to the change in time interval. In the supplementary material of the paper we show and comment the results for three different time windows:

1) **30years [2070 /2100 – 2006/2036] ,**
2) **40years [2060 /2100 – 2006/2046] ,**
3) **50years [2050 /2100 – 2006/2056] .**

Coherence among spatial structures is preserved although the intensity of changes is slightly different and generally increases by decreasing the window size. This is expected on the basis of the increased separation in the time periods considered.

Figure 7 in the supplementary summarizes with box-plots the addition requested by the referee. We report results for the two different scenarios, resolutions and time windows. It is interesting to

notice how the turbulent component ΔY changes with the resolution. We find that adding finer scales corresponds to richer turbulent contributions, as one would expect on theoretical basis.

Overall, we thank the referee for his comments and we believe that these additions increase the range of validity of our results.

Moreover, authors need to describe the wavelet-based approach, define what BIC is, and to explain how the parameters were chosen.

We added the BIC formula/explanation in the new version of the paper.

A wavelet-based-approach to detect climate change on the coherent and turbulent component of the atmospheric circulation

Davide Faranda[1] and Dimitri Defrance[1]

[1] LSCE-IPSL, CEA Saclay l'Orme des Merisiers, CNRS UMR 8212 CEA-CNRS-UVSQ, Université Paris-Saclay, 91191 Gif-sur-Yvette, France

Correspondence to: Davide Faranda (davide.faranda@lsce.ipsl.fr)

Abstract. The modifications of atmospheric circulation induced by anthropogenic effects are difficult to capture because wind fields feature a complex spectrum where the signal of large scale coherent structures (planetary, baroclinic waves and other long-term oscillations) is mixed up with turbulence. Our purpose is to study separately the effects of climate changes on these two components by applying a wavelet analysis to the 700 hPa wind fields obtained in climate simulations for different forcing scenarios. We study the coherent component of the signal via a correlation analysis to detect the persistence of large-scale or long-lasting structures, whereas we use the theory of Auto-Regressive Moving-Average stochastic processes to measure the spectral complexity of the turbulent component. Under strong anthropogenic forcing, we detect a significant climate-change signal. The analysis suggests that coherent structures will play a dominant role in future climate, whereas turbulent spectra will approach a classical Kolmogorov behavior.

1 Introduction

Scale separation is an essential property for the study of natural systems: Langrangian mechanics has been applied to the study of the solar system because planets appear so small that they can be considered as material points with respect to the length of their orbits (Murray and Dermott, 1999). In a less obvious framework, Einstein and Langevin recognized that the behavior of heavy particles in a gas can be studied by introducing two different scales: the inertial (slow) motion of the heavy particles and the interactions (fast) with the gas particles (Langevin, 1908). In geophysics the same approach has been - sometimes implicitly - applied for understanding important mechanisms driving the atmospheric and oceanic circulation: one can model the baroclinic instability because cyclones have a well determined size and their structure emerges out from the atmospheric turbulence (Charney, 1947), El Nino because of the precise time-scales involved in the phenomenon (Cane and Zebiak, 1985; Penland and Magorian, 1993). The success of a scale-separation based approach is due to the intrinsic properties of stratified and rotating flows. In homogeneous and isotropic turbulence, the energy flows towards the small scales and coherent structures are rapidly destroyed. This is the so-called direct cascade proposed in Kolmogorov (1941)). Instead, geophysical flows are stratified and rotational flows where an inverse cascade of energy induces the bidimensionalization of motions and contributes to the formation of large scale coherent structures (Pouquet and Marino, 2013). In laboratory experiments (Lamriben et al., 2011) and geophysical observations (Craig and Banner, 1994; Holmes et al., 1998) one aims at separating coherent and turbulent components and build theoretical models to describe the associated motions (Charney, 1971; Pitcher, 1977; Jiang et al., 1995; Lucarini et al., 2007). As pointed out by several authors (see Schertzer and Lovejoy (1991) for a review), this task is non-trivial because both the inverse and direct cascades coexist for geophysical motions. The direct cascade is eventually responsible for the dissipation of energy, the transfer of momentum from the atmosphere to the ocean and the soil, the disruption of large scale structures in the flow resulting in an unpredictable behavior (Leith, 1971). The inverse cascade contributes to the formation of cyclonic and anticyclonic structures observed in the atmosphere and the ocean. Morevoer, it generally enhances the predictability of future states of the atmosphere (Paladin and Vulpiani, 1994; Tribbia and Baumhefner, 2004).

In this paper we present two indicators that describe the statistical properties of large scale coherent structures as well as turbulent spectra, investigating their response to climate change. The indicators are defined after separating the coherent structures from featureless turbulence via the wavelet filtering technique. For the coherent part, we compute the integral of the auto-correlation function as a measure of the persistence of the coherent structure. For the turbulent component, we use an indicator that measures the complexity of the spectrum with respect to the canonical behavior theorized by Kolmogorov.

We test the technique on the horizontal wind data measured at 700hPa for two different anthropogenic emission scenarios (RCP 2.6 and 8.5). We investigate whether the anthropogenic and natural forcing could cause not only ~~change~~ a change in the intensity of some defined observable (as it is now evident for the global mean temperature), but also in the direction the energy is cascading and therefore in the relative importance of large scale coherent structure with respect to turbulence.

2 Methods

The separation between coherent $X(t)$ and turbulent $Y(t)$ components of a time series $Z(t)$ is done via wavelet filters (Farge, 1992). With respect to simple filtering technique (e.g. moving-average filters), the wavelet filters are useful when the time series contain multiple timescales and there is not a trivial scale separation. Wavelet analysis has been widely applied in climate science (Torrence and Compo, 1998) and to the analysis of geophysical time series (Ghil et al., 2002; Grinsted et al., 2004) . We give a brief illustration of the wavelet filtering technique by analyzing a time series of u_{500} taken from the scenario RCP 2.6 at the point lon 78W lat 38N. The series consisting of 512 monthly observations and it is shown in Fig. 1a). Its power spectral density (psd) is visualized in Fig. 1b. The series shows an evident periodic component (the seasonal cycle) captured by the spectral peak. The spectrum is compared with a flat one (dotted line) reproducing a perfect white noise signal. The results of the wavelet filter are shown in Fig.1c-f). The coherent component $X(t)$ and its spectrum are shown in Fig.1c,d) respectively. The effects of the filter are not directly visible on the detrended time series, but rather on the spectra. The psd for the coherent part of the signal presents a significant slope with the energy concentrated at large time scales. On the contrary, the incoherent component $Y(t)$ represented in Fig.1e) has a rather flat psd (Fig.1f), as expected from a ~~successfull~~ successful application of the technique. Nonetheless, the limits of the wavelet filtering approach appear by looking at the spectral peak corresponding to the seasonal cycle which cannot be completely eliminated, although it represents a coherent component of the signal.

Once the separation between coherent and noisy component is done, we study the property of $X(t)$ and $Y(t)$ separately. For the coherent component $X(t)$ we use as indicator the memory of the system by measuring the integral of the autocorrelation function defined as:

$$ACF(X)(\tau) = E[X(t)X^*(\tau)],$$

where $E[X]$ stands for expectation value. The ACF measures how long the system remember an initial condition. For a white noise signal, it decays to 0 as $\tau > 1$. For a correlated signal it decay slowly to 0 for large τ. For a perfectly periodic signal, the ACF is periodic itself. The integral of the ACF in its discrete version is written us:

$$\Lambda = \sum_{\tau=0}^{T} ACF(X)(\tau),$$

where we sum the correlation up to a time T sufficiently large for the ACF to decay to 0. Λ measures how long coherent structures persist in time and it is therefore linked to the predictability: the higher the correlation, the higher the probability that the structure will be preserved in future times (Schubert et al., 1992). The link between correlations decay and predictability is well known in dynamical systems theory and in physics (Osborne and Provenzale, 1989; Govindan et al., 1998; Crisanti et al., 1993) and we now exploit it to study properties of geophysical time series.

For the noisy component $Y(t)$ we use an indicator of the spectral complexity with respect to the canonical Kolmogorov behavior. In order to introduce this indicator we will use the class of Auto Regressive Moving Average stochastic processes. In general, a stationary time series Y_t of an observable with unknown underlying dynamics can be modeled by an ARMA(p,q) process such that for all t:

$$Y_t = \sum_{i=1}^{p} \phi_i Y_{t-i} + \varepsilon_t + \sum_{j=1}^{q} \theta_j \varepsilon_{t-j} \tag{1}$$

with $\varepsilon_t \sim WN(0,\sigma^2)$ - where WN stands for white noise - and the polynomials $\phi(z) = 1 - \phi_1 z_{t-1} - \cdots - \phi_p z_{t-p}$ and $\theta(z) = 1 - \theta_1 z_{t-1} - \cdots - \theta_q z_{t-q}$. Notice that, hereinafter, the noise term ε_t will be assumed to be a white noise, which is a very general condition (Box and Jenkins, 1970).

The basic model for the noisy component is the ARMA(1,0) or simply AR(1) model which is the simplest compatible with the Kolmogorov spectrum (Thomson, 1987). When the spectral complexity increases, the best ARMA model describing the velocity time series will deviate from the basic one. We can define a normalized distance between the reference ARMA($\overline{p}$, $\overline{q}$) and any other ARMA(p, q) ~~model as the~~ by using the Bayesian information criterion (BIC), which measures the relative quality of a statistical model, as:

$$BIC = -2\ln \hat{L}(n, \hat{\sigma}^2, p, q) + k[\ln(n) + \ln(2\pi)], \tag{2}$$

where $\hat{L}(n,\hat{\sigma}^2,p,q)$ is the likelihood function for the investigated model and in our case $k=p+q$ and n the length of the sample. The variance $\hat{\sigma}^2$ is computed from the sample and is a series-specific quantity.

Our indicator is a normalized difference between the $BIC(n,\hat{\sigma}^2,p+1,q)$ and the ARMA($\overline{p}$, $\overline{q}$) $BIC(n,\hat{\sigma}^2,\overline{p},\overline{q})$:

$$\Upsilon = 1-\exp\left\{|BIC(p+1,q)-BIC(\overline{p},\overline{q})|\right\}/n. \tag{3}$$

with $0\leq\Upsilon\leq 1$: it goes to zero if the dataset is well described by an ARMA($\overline{p}$, $\overline{q}$) model and tends to one in the opposite case.

We have ~~already~~ checked that such indicators perform well in different physical systems, ~~providing~~ and generally provide more information than the ~~usual ones , based on the critical slow down due to the increase of correlations in the systems at the transition. These analyses have been recently published~~ ones based on correlations analysis only. Such results can been found in (Faranda et al., 2014) where indicators similar to Υ have been used to model different physical systems: Ising and Langevin models and turbulence. A large Υ correspond to a complex spectrum with non-trivial scale-interactions and non-constant energy transfers, a small Υ correspond to a spectrum compatible with the Kolmogorov spectrum with constant energy fluxes between scales. The predictability will decrease with ~~an~~ a higher Υ because more structures at different scales will have to be followed to describe the behavior of the system. In other words, for high Υ the component $Y(t)$ cannot be just modelled as simple noise.

3 Analysis

We illustrate the potential of Λ and Υ indicators on a climate change experiment used in the CMIP5 framework for the IPCC AR5 report (Collins et al., 2013). To explore the climate change of the next century, the IPCC has developed four different scenarios, defined in terms of radiative evolution and corresponding to a concentration of greenhouse gases year by year between 2006 and 2100 and extended until 2300. Here we consider two scenarios: i) the low emission scenario (RCP2.6) leading to a radiative balance of 2.6 W/m2 in 2100 with a peak at 3W/m2 and a decreasing trend ii) the higher emission scenario (RCP8.5) predicting an increase up to 8.5W/m2 in 2100. The effect of such greenhouse gases perturbations are well known for some observables, e.g. the global temperature increase ranges from 1±0.4 °C to 3.7±0.7 °C in the last part of the period 2081-2100 (Collins et al., 2013).

We focus on the daily horizontal winds at 700 hPa (u_{700}, v_{700}) obtained from the IPSLCM5-LR model, where LR stands for low resolution. This model is developed by the Institut Pierre-Simon Laplace with several laboratories. It consists of several components : atmosphere (LMDZ), ocean (NEMO), continent (ORCHIDEE) and sea-ice (LIM). For LMDZ ~~, a spatially resolution is of~~ and ORCHIDEE, the spatial resolution is 3.75° X 1.875° in longitude and latitude respectively with 39 vertically levels~~and, for NEMO, a spatially resolution~~ . For NEMO, the resolution is of about 2°, with a higher latitudinal resolution of 0,5° in the equatorial ocean, and 31 ~~vertically~~ vertical levels. ORCHIDEE takes into account the evolution of the lands (urbanization, forests, agriculture) (Dufresne et al., 2013). We chose the 700 hPa (about 3km) because it has been recognized as the best level for tracking the coherent atmospheric structures as shortwaves, extra-tropical cyclones and convective storms, since they are all advected, in first approximation, by 700 hPa horizontal winds (Mölders and Kramm, 2014). We have also performed robustness tests by considering the Medium Resolution (MR) version of the IPSLCM5 model (2.5° X 1.25° in longitude and latitude for LMDZ and ORCHIDEE while the resolution of other models is the same as LR). These tests are reported and explained in the supplementary material.

We begin the analysis by showing typical maps of Λ and Υ for the scenario RCP 2.6 and the two components: the zonal u_{700} and the meridional v_{700} (Fig. 2). Λ shows, for the zonal component, a rich structure with several areas where persistent coherent structures are well identified (Fig. 2a). Because we are using daily time series, the values of Λ can be directly interpreted as the number of days of persistence of these structures. At the mid-latitudes, the signature of stationary planetary waves is visible. In correspondence to the location of such waves, we find $\Lambda \sim$16 days, a value compatible with the work of Torrence and Compo (1998) who studied planetary waves using other indicators based on the wavelet approach. ~~At~~ In the tropics, the high values of Λ can be linked to the easterly jets (Koteswaram, 1958). The core of the African easterly jet is located about at this level (Nicholson, 2009), as well as for the Choco and Caribbean low level jets (Wang, 2007). The results for Λ computed on the meridional component v_{700} are shown in Fig. 2c). Here the largest values are found in correspondence of the regions affected by monsoons. The strongest signal is for the African monsoon because the IPSL model localizes it better than the Indian one (Dufresne et al., 2013). At the mid-latitudes the patches visible near the Pacific coast and over USA correspond to areas where the zonal flow is blocked by the Rocky Mountains and meridional winds blow to allow the flows go round the mountains.

For the Υ analysis, there is not much difference ~~ibn~~ in the structure of the zonal component (Fig. 2b) and the meridional component (Fig. 2d). The spatial pattern of Υ can be explained in light of the tropical atmospheric dynamics. Higher values are located on the tropics, where ~~convective storms are the major actor in determining the weather. The non-trivial interplay between deep convection and other meteorological turbulent phenomena affecting the tropics is responsible for high Υ values.~~ turbulence is associated to the convective activity in the area. We remark that, as the resolution is increased, the $\Delta\Upsilon$ increases (see supplementary Figure 7). This means that turbulent contribution becomes more relevant when finer scales are included in the analysis, although the scale of the analysis remains, even in the MR simulation, much larger than the scales of convective structures ($\sim$ 10 Km).

We now investigate whether Λ and Υ can detect changes in the coherent or noisy components of the 700 hPa horizontal winds under the climate change RCP 2.6 and RCP 8.5 scenarios. We divide the daily time series in two period: 2005-2055 and 2055-2105 and compute the quantities: $\Delta\Lambda = \Lambda_{2055-2105} - \Lambda_{2005-2055}$ and $\Delta\Upsilon = \Upsilon_{2055-2105} - \Upsilon_{2005-2055}$. For both the indicators, the RCP 8.5 scenario shows considerable impacts, whereas the changes for the RCP 2.6 are appreciable only for the u_{700} component. In the supplementary material, we report the results also for time windows of 30 and 40 years. By decreasing the time window considered, we observe that the spatial structure of $\Delta\Lambda$ and $\Delta\Upsilon$ does not change (Supplementary Figures 1-6). However, the changes in the indicator become locally sharper as shorter time windows are considered, as one would expect by taking differences of periods with a larger time separation (Supplementary Figure 7).

The $\Delta\Lambda$ fields for the u_{700} and the v_{700} components present interesting structures: the strongest signals are located over the Pacific ocean in correspondence of the El Nino Region 3 (for u_{700}) and Region 3.4 for v_{700}, described in Trenberth (1997). At the ~~midlatitudes~~mid-latitudes, dipolar structures appear both for the zonal and for the meridional flow (Barnston et al., 1997). This is the signature of the jet stream shift observed by several studies. For the northern hemisphere, changes in the pattern of meridional winds are ~~highlited by an alternance~~ highlighted by an alternation of negative and positive $\Delta\Lambda$: we can link these changes to the modification in stationary planetary waves associated to the change in the jet streams intensity and positions. Several studies have recently appeared on this issue, although is not clear whether the cause can be linked to the so-called Artic amplification (Serreze and Francis, 2006), rather than to changes in El Nino Southern Oscillation (Moritz et al., 2002), or even to the stratospheric dynamics (Serreze and Barry, 2011). $\Delta\Lambda$ also suggests that some regions will experience an increasing persistence of meridional winds i.e. an increasing of blocking conditions (e.g. central USA, western Europe), whereas some other areas will have an increase in the persistence of the zonal winds (e.g; Eastern Europe, Alberta (CA)).

The results for $\Delta\Upsilon$ indicates that the spectral complexity in the tropical regions tends to reduce ~~of~~ by about 10% ($\Delta\Upsilon \sim -0.1$) in the RCP 8.5 scenario. ~~A~~ Although the model does not resolve the convective scales, a possible explanation for this result relies on the enhanced convective activity resulting from the sea surface warming and resulting in an increase of precipitations in the area, as we have verified for the IPSL model and reported by other studies (Huang et al., 2013). This consideration is true only if convective parametrization transfers energy from the convective scales to the scale of the analysis. In other words, at the actual resolution of climate models we can just observe the footprints of these phenomena. If turbulence becomes stronger and anisotropic, then it should approach the Kolmogov behavior, and Υ should tend to 0.

4 Conclusions

We have devised two indicators to study the changes in the atmospheric circulation by separating the coherent structures from the turbulent part of the signals. The indicator for the coherent structures $\Delta\Lambda$ is a measure of the total persistence of the coherent structure, whereas $\Delta\Upsilon$ is a measure of the residual complexity of the turbulent spectrum, once the coherent component has been removed.

The indicators show significant changes when the climate system is subject to greenhouse gases forcing. The difference in the indicators for the RCP 8.5 scenario between the second half and the first half of the 21st century suggests that El Nino Southern Oscillation will play a major role and blocking conditions will change the typical coherent structures observed at the mid-latitude.

Besides the regional patterns, we believe that the most important message is contained in the global average of our indicators. For the RCP 8.5 scenario, $\Delta\Lambda$ increases by 0.5 days in the second half of the century for u_{700} and by 0.2 days for v_{700}. On the other hand, the spectral complexity decreases in the tropical regions of about 10%. This suggests that the coherent structures will play a major role in the atmospheric dynamics and this will probably enhance the predictability of the atmosphere on weekly to monthly time-scales. The contrast between these two effects could be one of the causes of the difficulty in finding significant traces of climate change in the circulation dynamics, a problem recently highlighted by Shepherd (2014).

Our indicators have been here illustrated for a single model at two different spatial resolutions and in two climate change scenarios. They could be useful to evaluate the response of atmospheric circulation to changes in the forcing for several models. Moreover the technique does not require the variables to be velocity fields and it could be extended to any physical time series in which a non-trivial scale separation is present.

Acknowledgements. D. Faranda was supported by ERC grant No. 338965-A2C2. DD was supported by the French Atomic Commission (CEA) within the framework of the VACCIN project (Variations Abruptes du Climat: Conséquences et Impacts éNergétiques) funded by the DSM-Energie Program. It benefited from the HPC resources made available by GENCI (Grand Equipement National de Calcul Intensif), CEA and CNRS (Centre National de la Recherche Scientifique).

References

Barnston, A. G., Chelliah, M., and Goldenberg, S. B.: Documentation of a highly ENSO-related SST region in the equatorial Pacific, Atmosphere-ocean, 35, 367–383, 1997.

Box, G. E. and Jenkins, G. M.: Time Series Analysis: Forecasting and Control., Holden-D. iv, 1970.

Cane, M. A. and Zebiak, S. E.: A theory for El Nino and the Southern Oscillation, Science, 228, 1085–1087, 1985.

Charney, J. G.: The dynamics of long waves in a baroclinic westerly current, Journal of Meteorology, 4, 136–162, 1947.

Charney, J. G.: Geostrophic turbulence, Journal of the Atmospheric Sciences, 28, 1087–1095, 1971.

Collins, M., Knutti, R., Arblaster, J., Dufresne, J., Fichefet, T., Friedlingstein, P., Gao, X., Gutowski, W., Johns, T., Krinner, G., et al.: Climate change 2013: the physical science basis. Contribution of Working Group I to the Fifth Assessment Report of the Intergovernmental Panel on Climate Change, Long-term Climate Change: Projections, Commitments and Irreversibility, Cambridge Univ. Press, Cambridge, UK, and New York, 2013.

Craig, P. D. and Banner, M. L.: Modeling wave-enhanced turbulence in the ocean surface layer, Journal of Physical Oceanography, 24, 2546–2559, 1994.

Crisanti, A., Jensen, M., Vulpiani, A., and Paladin, G.: Intermittency and predictability in turbulence, Physical review letters, 70, 166, 1993.

Dufresne, J.-L., Foujols, M.-A., Denvil, S., Caubel, A., Marti, O., Aumont, O., Balkanski, Y., Bekki, S., Bellenger, H., Benshila, R., et al.: Climate change projections using the IPSL-CM5 Earth System Model: from CMIP3 to CMIP5, Climate Dynamics, 40, 2123–2165, 2013.

Faranda, D., Pons, F. M. E., et al.: Statistical early-warning indicators based on autoregressive moving-average models, Journal of Physics A: Mathematical and Theoretical, 47, 252 001, 2014.

Farge, M.: Wavelet transforms and their applications to turbulence, Annual review of fluid mechanics, 24, 395–458, 1992.

Ghil, M., Allen, M., Dettinger, M., Ide, K., Kondrashov, D., Mann, M., Robertson, A. W., Saunders, A., Tian, Y., Varadi, F., et al.: Advanced spectral methods for climatic time series, Reviews of geophysics, 40, 2002.

Govindan, R., Narayanan, K., and Gopinathan, M.: On the evidence of deterministic chaos in ECG: Surrogate and predictability analysis, Chaos: An Interdisciplinary Journal of Nonlinear Science, 8, 495–502, 1998.

Grinsted, A., Moore, J. C., and Jevrejeva, S.: Application of the cross wavelet transform and wavelet coherence to geophysical time series, Nonlinear processes in geophysics, 11, 561–566, 2004.

Holmes, P., Lumley, J. L., and Berkooz, G.: Turbulence, coherent structures, dynamical systems and symmetry, Cambridge university press, 1998.

Huang, P., Xie, S.-P., Hu, K., Huang, G., and Huang, R.: Patterns of the seasonal response of tropical rainfall to global warming, Nature Geoscience, 6, 357–361, 2013.

Jiang, S., Jin, F.-F., and Ghil, M.: Multiple equilibria, periodic, and aperiodic solutions in a wind-driven, double-gyre, shallow-water model, Journal of Physical Oceanography, 25, 764–786, 1995.

Kolmogorov, A. N.: Dissipation of energy in locally isotropic turbulence, in: Dokl. Akad. Nauk SSSR, vol. 32, pp. 16–18, 1941.

Koteswaram, P.: The easterly jet stream in the tropics, Tellus, 10, 43–57, 1958.

Lamriben, C., Cortet, P.-P., and Moisy, F.: Direct measurements of anisotropic energy transfers in a rotating turbulence experiment, Physical review letters, 107, 024 503, 2011.

Langevin, P.: Sur la théorie du mouvement brownien, CR Acad. Sci. Paris, 146, 1908.

Leith, C.: Atmospheric predictability and two-dimensional turbulence, Journal of the Atmospheric Sciences, 28, 145–161, 1971.

Lucarini, V., Speranza, A., and Vitolo, R.: Self-scaling of the statistical properties of a minimal model of the atmospheric circulation, in: Nonlinear Dynamics in Geosciences, pp. 197–219, Springer, 2007.

Mölders, N. and Kramm, G.: Lectures in Meteorology, Springer, 2014.

Moritz, R. E., Bitz, C. M., and Steig, E. J.: Dynamics of recent climate change in the Arctic, Science, 297, 1497–1502, 2002.

Murray, C. D. and Dermott, S. F.: Solar system dynamics, Cambridge university press, 1999.

Nicholson, S. E.: A revised picture of the structure of the "monsoon" and land ITCZ over West Africa, Climate Dynamics, 32, 1155–1171, 2009.

Osborne, A. R. and Provenzale, A.: Finite correlation dimension for stochastic systems with power-law spectra, Physica D: Nonlinear Phenomena, 35, 357–381, 1989.

Paladin, G. and Vulpiani, A.: Predictability in spatially extended systems, Journal of Physics A: Mathematical and General, 27, 4911, 1994.

Penland, C. and Magorian, T.: Prediction of Nino 3 sea surface temperatures using linear inverse modeling, Journal of Climate, 6, 1067–1076, 1993.

Pitcher, E. J.: Application of stochastic dynamic prediction to real data, Journal of the Atmospheric Sciences, 34, 3–21, 1977.

Pouquet, A. and Marino, R.: Geophysical turbulence and the duality of the energy flow across scales, Physical review letters, 111, 234 501, 2013.

Schertzer, D. and Lovejoy, S.: Nonlinear variability in geophysics, Springer, 1991.

Schubert, S. D., Suarez, M. J., and Schemm, J.-K.: Persistence and predictability in a perfect model, Journal of the atmospheric sciences, 49, 256–269, 1992.

Serreze, M. C. and Barry, R. G.: Processes and impacts of Arctic amplification: A research synthesis, Global and Planetary Change, 77, 85–96, 2011.

Serreze, M. C. and Francis, J. A.: The Arctic amplification debate, Climatic Change, 76, 241–264, 2006.

Shepherd, T. G.: Atmospheric circulation as a source of uncertainty in climate change projections, Nature Geoscience, 2014.

Thomson, D.: Criteria for the selection of stochastic models of particle trajectories in turbulent flows, Journal of Fluid Mechanics, 180, 529–556, 1987.

Torrence, C. and Compo, G. P.: A practical guide to wavelet analysis, Bulletin of the American Meteorological society, 79, 61–78, 1998.

Trenberth, K. E.: The definition of el nino, Bulletin of the American Meteorological Society, 78, 2771–2777, 1997.

Tribbia, J. and Baumhefner, D.: Scale interactions and atmospheric predictability: An updated perspective, Monthly weather review, 132, 703–713, 2004.

Wang, C.: Variability of the Caribbean low-level jet and its relations to climate, Climate dynamics, 29, 411–422, 2007.

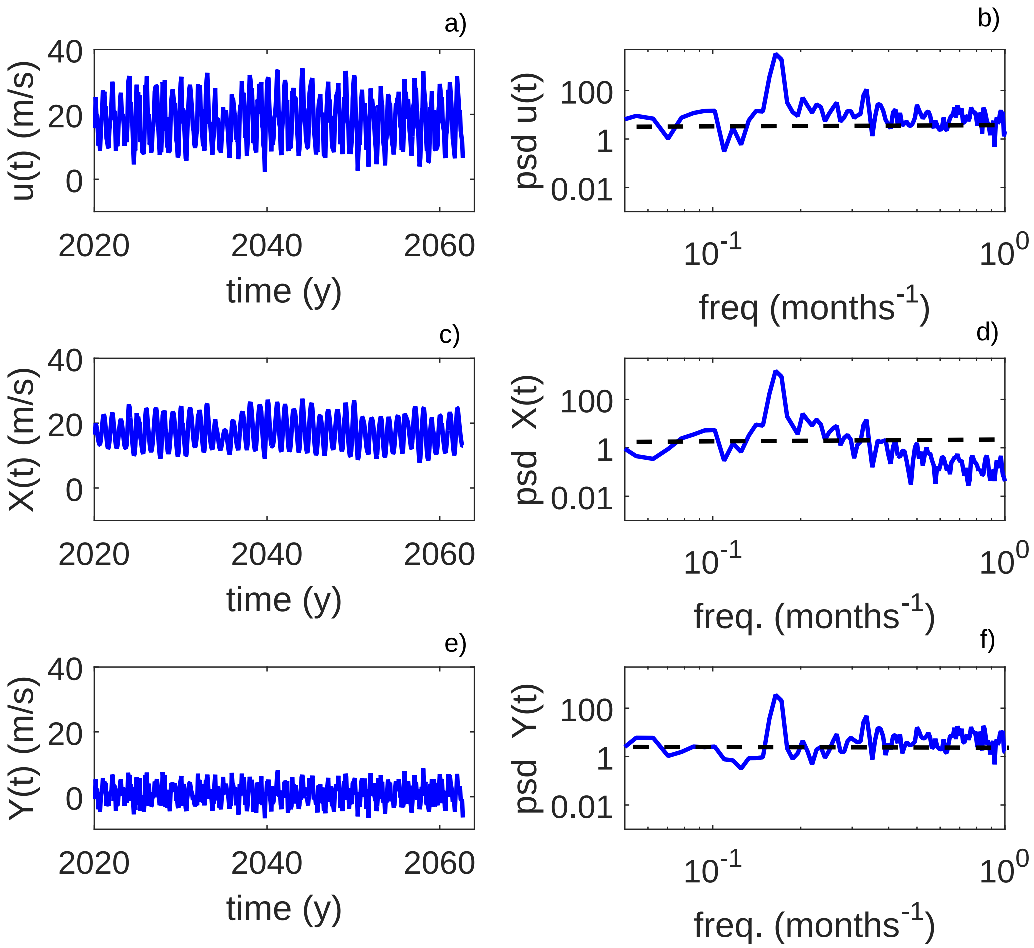

Figure 1. Example of wavelet filtering. a) u_{500} monthly time series at Lon=78W and Lat=38N and b) corresponding power spectral density (psd). c) Time series of the coherent component $X(t)$ extracted by the wavelet filter and d) its psd. e) Time series of the noisy component $Y(t)$ extracted by the wavelet filter and f) its psd.

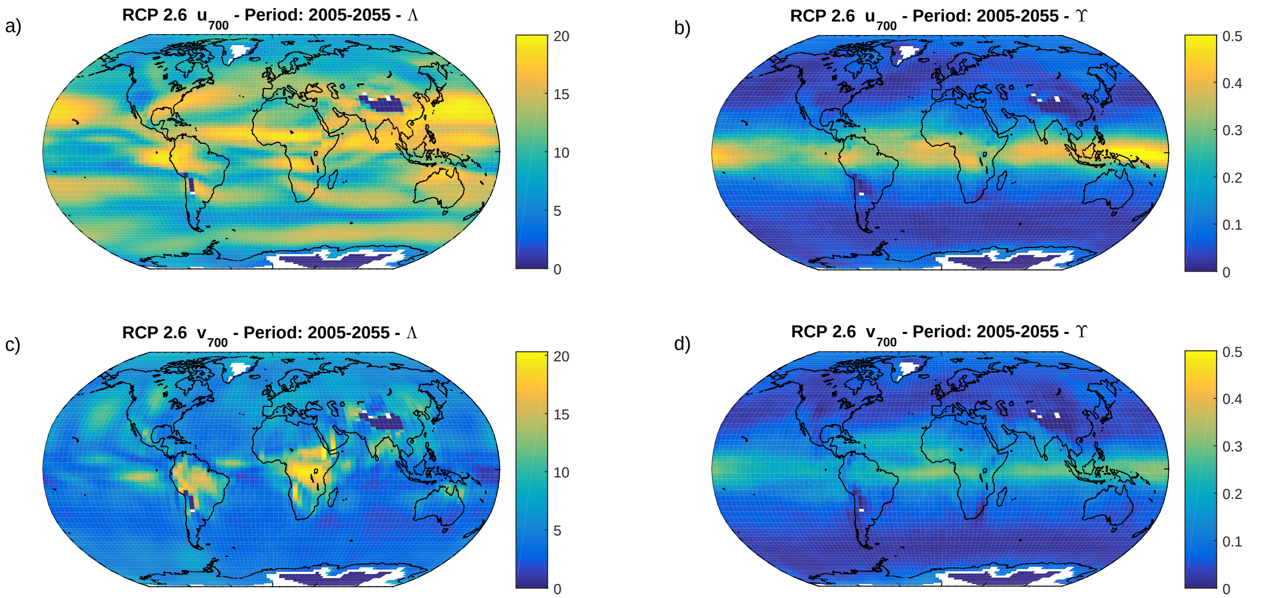

Figure 2. Integral of the autocorrelation function Λ for the period 2005-2055 for the u_{700} a) and for the v_{700} c) daily time series. Spectral complexity Υ for the period 2005-2055 for the u_{700} b) and for the v_{700} d) daily time series.

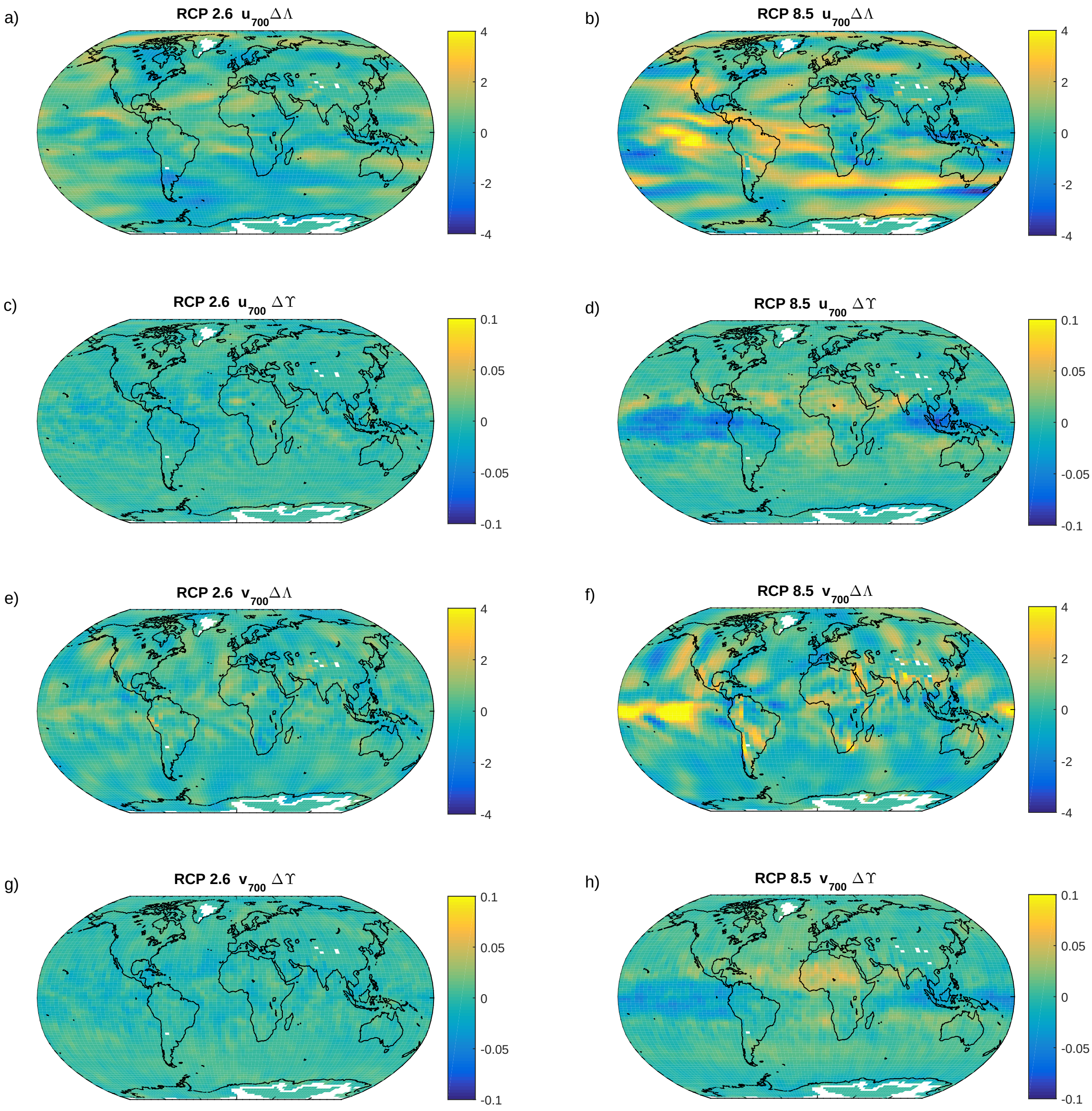

Figure 3. Differences in the integral of the autocorrelation function $\Delta\Lambda$ for the 2055-2105 and the 2005-2055 period for the u_{700} in the RCP 2.6 a) and in the RCP 8.5 b). Differences in the Spectral complexity $\Delta\Upsilon$ for the 2055-2105 and the 2005-2055 period for the u_{700} in the RCP 2.6 c) and RCP 8.5 d) scenario. $\Delta\Lambda$ for v_{700} for the RCP 2.6 e) and the RCP 8.5 f) scenarios. $\Delta\Upsilon$ for the v_{700} in the RCP 2.6 g) and RCP 8.5 h) scenario.